

# Extension of QSQH theory of scale interaction in near-wall turbulence to all velocity components

Sergei Chernyshenko†

Department of Aeronautics, Imperial College London, London SW7 2AZ, UK

(Received xx; revised xx; accepted xx)

An extension of the QSQH theory is proposed. It takes into account the fluctuations of the large-scale component of the wall friction. The extended theory applies to all three velocity components of near-wall turbulent flows. It explains the large sensitivity of the fluctuations of longitudinal and spanwise velocities to variations in the Reynolds number in comparison with the sensitivity of the mean velocity profile, the Reynolds stress, and the wall-normal velocity fluctuations. The analysis shows that the variation of the longitudinal velocity fluctuations with the Reynolds number is dominated by the variation of the amplitude and wall-normal-scale modulation of the universal mean velocity profile by the outer, large-scale, Reynolds-number-dependent motions. The variation of spanwise velocity fluctuations is dominated by the fluctuations of the direction of the large-scale component of the wall friction. The Reynolds number dependence of the other second moments is not dominated by these mechanisms because the mean wall-normal velocity and the mean spanwise velocity are zero. In particular, for a plane channel flow at the friction Reynolds number in the range of a few thousands the effect of the variation of the mean pressure gradient with the Reynolds number is stronger than the QSQH mechanisms as far as the variation of the Reynolds stress is concerned. The paper also covers the approximate nature of the QSQH theory and the advantages of using the units and variables of the QSQH theory instead of the wall units when the effect of large-scale motions on the near-wall turbulence is relevant.

## 1. Introduction

The modern understanding of near-wall turbulence has been largely built on the basis of the classical universality hypothesis, according to which as the Reynolds number,  $Re$ , tends to infinity, the characteristics of the near-wall part of a turbulent boundary layer, if expressed in wall units, become independent of  $Re$  and other factors such as the pressure gradient. However, research in the last two decades has shown that this hypothesis is at least inaccurate. High- $Re$  turbulent near-wall flows exhibit two peaks in the turbulent kinetic energy profile (see e.g. Smits *et al.* 2011). The first peak is located in the buffer layer, while the distance from the wall to the second, “outer”, peak varies with  $Re$ . The outer peak is caused by turbulent fluctuations at characteristic length scales that are significantly larger than those causing the inner peak (Hutchins & Marusic 2007). These outer large-scale motions and the inner small-scale motions located in the near-wall region interact (Rao *et al.* 1971; Mathis *et al.* 2009; Ganapathisubramani *et al.* 2012). Marusic *et al.* (2010) proposed the widely known empirical relation describing this interaction.

Since the large-scale motions are not  $Re$ -independent if expressed in wall-units, the scale interaction invalidates the classical universality hypothesis. The recently developed

† Email address for correspondence: s.chernyshenko@imperial.ac.uk

Quasi-Steady-Quasi-Homogeneous (QSQH) theory (Chernyshenko *et al.* 2012; Zhang & Chernyshenko 2016; Chernyshenko *et al.* 2019) remedies this. In essence, the QSQH hypothesis states that the small-scale near-wall motions adapt to the large-scale fluctuations of the wall shear stress.

Results agreeing to various degree with the QSQH theory were obtained in (Chernyshenko *et al.* 2012; Agostini & Leschziner 2014, 2018; Zhang & Chernyshenko 2016; Baars *et al.* 2016, 2017; Agostini *et al.* 2017; Howland & Yang 2018; Chernyshenko *et al.* 2019; Zhang 2019; Agostini & Leschziner 2019a; Lozier *et al.* 2019). The theory was performed better for higher  $Re$  and smaller distances to the wall. In most cases, significant deviations occurred only for  $y^+ > 70$  wall units.

Agostini & Leschziner (2019b) attempted to extend the QSQH theory stated originally for the longitudinal velocity only, to the spanwise and wall-normal velocity components, and found that while for the wall distance  $y^+ < 70$  the behaviour of the longitudinal,  $u$ , and wall-normal,  $v$ , velocity components was in approximate agreement with their extension of the QSQH theory, the behaviour of the spanwise velocity component  $w$  was in a noticeable disagreement even in the close vicinity of the wall. They attributed this discrepancy to the effect of the wall-normal component of the large-scale motions, but also mentioned that taking into account that the wall friction is a vector, as suggested by Zhang & Chernyshenko (2016), might improve the performance of the theory. The observed discrepancy is intriguing because velocity components are related by the continuity equation and, at a first glance, an agreement in two components should lead to an agreement in the third component.

Research involving comparisons for all three velocity components is likely to be continuing. It is therefore timely to provide the formulation of the QSQH theory taking into account the fluctuation of the direction of the large-scale wall friction. This is the main goal of the present paper. First results within the extended theory and a brief discussion will also be presented.

## 2. Extension of the QSQH theory to all velocity components

We assume that there is a suitable definition of large scales and small scales. Let the wall friction be represented as a sum of the large-scale and small-scale components:  $\tau^* = \tau_L^* + \tau_S^*$ . If the large-scale component  $\tau_L^*$  were independent of time, while the small-scale component had zero time average, one could use wall units based on  $\tau_L^*$ , which would coincide with the time-averaged wall friction, and expect that near the wall the flow statistics expressed in wall units would be (approximately) independent of  $Re$  and other factors, including  $\tau_L^*$ . The QSQH theory assumes that the same remains true even when  $\tau_L^*$  is dependent on time and the wall-parallel coordinates. Physical meaning of this hypothesis is therefore that the near-wall flow adjusts to the large-scale wall friction as if it were constant in time and homogeneous in space.

In the rest of the paper all quantities will be made non-dimensional using the kinematic viscosity  $\nu^*$  and the average magnitude of the large-scale friction velocity  $\langle u_{\tau_L}^* \rangle = \langle \sqrt{|\tau_L^*(t, x, z)|/\rho^*} \rangle$ , where  $\rho^*$  is the density and the angular brackets denote averaging. In these units  $\langle u_{\tau_L}^* \rangle = 1$ . The commonly used wall units based on  $\langle \tau^*(t, x, z) \rangle$  and  $\nu^*$  are very close quantitatively, at least for moderate  $Re$ , when the fluctuations of the magnitude of large-scale motions are small.

The large-scale component of the wall friction  $\tau_L(t, x, z)$  is a vector. A local coordinate system with an axis along the direction of  $\tau_L(t, x, z)$  shown in figure 1 and the coordinate

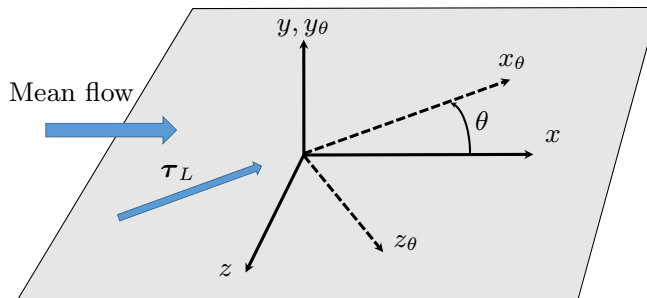


FIGURE 1. The coordinate systems:  $x$  is in the direction of the mean flow,  $x_\theta$  is in the direction of the large-scale component of the wall friction,  $y$  and  $y_\theta$  coincide, being in the wall-normal direction,  $z$  and  $z_\theta$  are in the wall plane and perpendicular to  $x$  and  $x_\theta$  respectively. The angle  $\theta$  is measured clockwise if looked at from above the wall.

system  $x, y, z$  aligned with the mean flow direction are related by the formulae

$$x_\theta = x \cos \theta - z \sin \theta, \quad y_\theta = y, \quad z_\theta = x \sin \theta + z \cos \theta, \quad (2.1)$$

$$u = u_\theta \cos \theta + w_\theta \sin \theta, \quad v = v_\theta, \quad w = -u_\theta \sin \theta + w_\theta \cos \theta. \quad (2.2)$$

Note that the angle  $\theta$  between the large-scale friction direction and the mean friction direction is a “large-scale” parameter.

The main relationships of the extended QSQH theory are

$$u_\theta(t, x_\theta, y_\theta, z_\theta, Re) = u_{\tau_L} \tilde{u}(\tilde{t}, \tilde{x}, \tilde{y}, \tilde{z}), \quad (2.3)$$

$$v_\theta(t, x_\theta, y_\theta, z_\theta, Re) = u_{\tau_L} \tilde{v}(\tilde{t}, \tilde{x}, \tilde{y}, \tilde{z}), \quad (2.4)$$

$$w_\theta(t, x_\theta, y_\theta, z_\theta, Re) = u_{\tau_L} \tilde{w}(\tilde{t}, \tilde{x}, \tilde{y}, \tilde{z}), \quad (2.5)$$

$$\tilde{t} = tu_{\tau_L}^2, \quad \tilde{x} = x_\theta u_{\tau_L}, \quad \tilde{y} = y_\theta u_{\tau_L}, \quad \tilde{z} = z_\theta u_{\tau_L}. \quad (2.6)$$

Even though (2.3-2.6) do not involve  $\theta$ , the statistics of  $u$ ,  $v$ , and  $w$  depend on the statistics of  $\theta$  since it enters (2.1,2.2).

If  $u_{\tau_L}$  and  $\theta$  were independent of time then  $u_{\tau_L}$  would be equal to 1, the averaged large-scale friction would be equal to the mean friction, our non-dimensional units would coincide with the wall units,  $\tilde{u}, \tilde{v}, \tilde{w}$  would be the velocity components in wall units  $u^+, v^+, w^+$ , and  $\tilde{t}, \tilde{x}, \tilde{y}, \tilde{z}$  would be the time and coordinates in wall units  $t^+, x^+, y^+, z^+$ . Equations (2.3-2.6) are the QSQH theory refinement suggested, although not explicitly formulated, by Zhang & Chernyshenko (2016). If only the magnitude of the wall friction but not its direction fluctuates, that is  $\theta = 0$ , then (2.3) coincides with (5) in Chernyshenko *et al.* (2012), and (2.4,2.5) are the assumptions implied by Agostini & Leschziner (2019b).

Many applications of the QSQH theory require large scales to be defined. Zhang & Chernyshenko (2016) circumvented this by specifying only a few properties of the large-scale filter,  $L$ , that, applied to the total field, gives the large-scale component of this field. For completeness, we list these properties here. For any constants  $a$  and  $b$  and functions  $f(t, x, y, z)$  and  $g(t, x, y, z)$ : (i)  $L(af + bg) = aL f + bL g$  (linearity), (ii)  $L \langle f \rangle = \langle f \rangle$  (invariance of averages: the averaged variables are large-scale), (iii)  $LL f = L f$  (projection property: the large-scale filter does not change an already large-scale-filtered function), (iv)  $\langle L f \rangle = L \langle f \rangle$  (commuting with averaging), and (v) scale-separation property: applying the large-scale filter to any function of  $t, x, y, z$  and other arguments that are large-scale-filtered variables is equivalent to averaging over the

homogeneous directions and/or time  $t, x$ , and  $z$  with the other arguments held constant:  $\mathbb{L} f(t, x, y, z, Lg_1, \dots, Lg_n) = \langle f(t, x, y, z, \xi_1, \dots, \xi_n) \rangle_{\xi_1=Lg_1, \dots, \xi_n=Lg_n}$ .

The important fifth property expresses the reason why the QSQH theory might describe the scale interaction in near-wall turbulence. Property (v) will be satisfied to the extent to which the characteristic dimensions of the large scales are much larger than the characteristic dimensions of small scales. Since turbulent flows have a continuum spectrum, the largest small-scale motions cannot be much smaller than the smallest large-scale motions. Hence, for turbulent flows the QSQH theory is only approximate even as  $Re$  tends to infinity. The quality of its predictions depends on how well the large-scale filter used by the researcher satisfies the fifth property.

The full statement of the 3D QSQH theory consists of: relations (2.3-2.5), the assumptions that for  $\tilde{t}, \tilde{x}, \tilde{y}$ , and  $\tilde{z}$  held constant,  $(\tilde{u}(\tilde{t}, \tilde{x}, \tilde{y}, \tilde{z}), \tilde{v}(\tilde{t}, \tilde{x}, \tilde{y}, \tilde{z}), \tilde{w}(\tilde{t}, \tilde{x}, \tilde{y}, \tilde{z}))$  and  $(u_{\tau_L}, \theta)$  are statistically independent, and that, also for  $\tilde{t}, \tilde{x}, \tilde{y}$ , and  $\tilde{z}$  held constant, the statistical properties of  $(\tilde{u}(\tilde{t}, \tilde{x}, \tilde{y}, \tilde{z}), \tilde{v}(\tilde{t}, \tilde{x}, \tilde{y}, \tilde{z}), \tilde{w}(\tilde{t}, \tilde{x}, \tilde{y}, \tilde{z}))$  and  $(u_{\tau_L}, \theta)$  are independent of  $Re$  and other large-scale factors such as the steady pressure gradient or smooth wall curvature, and the five properties of the large-scale filter, of which (v) is particularly significant.

If only the statistics that are one-point in wall-parallel directions and time are considered, shifting the coordinate origin to the point and time of interest makes  $t = x = x_\theta = z = z_\theta = 0$ . Then with zero arguments omitted (2.1-2.5) reduce to

$$u/u_{\tau_L} = \tilde{u}(yu_{\tau_L}) \cos \theta + \tilde{w}(yu_{\tau_L}) \sin \theta, \quad (2.7)$$

$$v/u_{\tau_L} = \tilde{v}(yu_{\tau_L}), \quad (2.8)$$

$$w/u_{\tau_L} = -\tilde{u}(yu_{\tau_L}) \sin \theta + \tilde{w}(yu_{\tau_L}) \cos \theta. \quad (2.9)$$

Further considerations in the present paper will refer to this case.

Typical application of the QSQH theory involves expressing the flow statistics in terms of the statistics of the universal velocity  $(\tilde{u}, \tilde{v}, \tilde{w})$  and the statistics of  $u_{\tau_L}$  and  $\theta$ . The relevant techniques can be illustrated with the simple example of mean velocity. From (2.7),  $U(y) = \langle u(y) \rangle = \langle u_{\tau_L} (\tilde{u}(yu_{\tau_L}) \cos \theta + \tilde{w}(yu_{\tau_L}) \sin \theta) \rangle$ . From the filter properties (ii) and (iv) it follows that  $\langle f \rangle = \langle \mathbb{L} f \rangle$  for any  $f$ . Hence,  $U(y) = \langle \mathbb{L} u_{\tau_L} (\tilde{u}(yu_{\tau_L}) \cos \theta + \tilde{w}(yu_{\tau_L}) \sin \theta) \rangle$ . By property (v),  $\mathbb{L} u_{\tau_L} \tilde{u}(yu_{\tau_L}) \cos \theta = u_{\tau_L} \tilde{U}(yu_{\tau_L}) \cos \theta$ , where  $\tilde{U}(\tilde{y}) = \langle \tilde{u}(\tilde{y}) \rangle$ . Note that  $\tilde{W}(\tilde{y}) = \langle \tilde{w}(\tilde{y}) \rangle = 0$  from symmetry. Finally,  $U(y) = \langle u_{\tau_L} \tilde{U}(yu_{\tau_L}) \cos \theta \rangle$ . For  $Re$  achievable so far in direct numerical simulations the amplitude of the fluctuation of large-scale motions is small. Constructing a truncated Taylor expansion in powers of  $\theta$  and  $u'_{\tau_L} = u_{\tau_L} - 1$  or their statistical moments is fruitful, but requires a caution in determining the sufficient number of terms. For the mean velocity it gives

$$U(y) = \tilde{U}(y) + \langle u_{\tau_L}^2 \rangle \frac{d}{dy} \frac{y^2}{2} \frac{d\tilde{U}}{dy} - \langle \theta^2 \rangle \frac{\tilde{U}(y)}{2} + \dots \quad (2.10)$$

This completes a brief description of the theory including the properties of the filter and the ideas of the main techniques used in the applications. Now we will show that taking into account the fluctuations of the direction of large-scale friction makes a difference.

### 3. Dependence of mean velocity and second moments on $Re$

#### 3.1. Sensitivity of mean velocity and the second moments to changes in $Re$

It is known but remained unexplained so far that both in absolute and in relative terms the variation of  $u_{\text{rms}}^2 = \langle u'^2 \rangle$  and  $w_{\text{rms}}^2 = \langle w'^2 \rangle$  with  $Re_\tau$  is much greater than

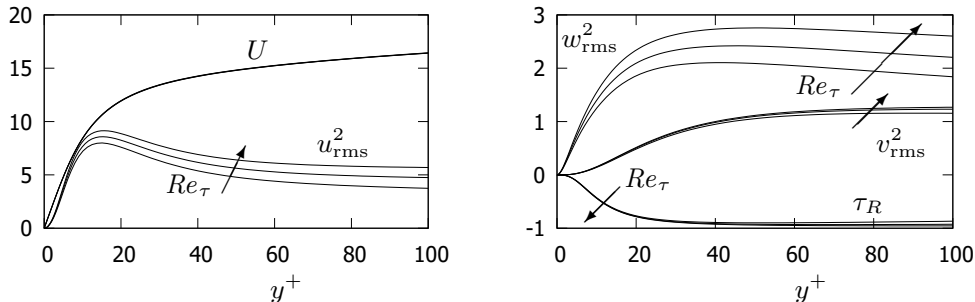


FIGURE 2. The DNS data for  $Re_\tau = 950, 2000$  and  $5200$  showing that  $u_{\text{rms}}^2$  and  $w_{\text{rms}}^2$  vary with  $Re_\tau$  significantly more than  $U$ ,  $v_{\text{rms}}^2$  and  $\tau_R = \langle u'v' \rangle$ . The three curves for  $U$  overlap.

the variation of  $U(y)$ ,  $v_{\text{rms}}^2 = \langle v'^2 \rangle$ , and the Reynolds stress  $\tau_R = \langle u'v' \rangle$  (see figure 2).<sup>†</sup> Applying the same technique as used to derive (2.10) and using the natural assumption that  $\tilde{V}(\tilde{y}) = \langle \tilde{v}(\tilde{y}) \rangle = 0$  and  $\tilde{W}(\tilde{y}) = \langle \tilde{w}(\tilde{y}) \rangle = 0$  gives

$$u_{\text{rms}}^2(y) = \tilde{u}_{\text{rms}}^2(y) + \langle u_{\tau_L}^{\prime 2} \rangle \left[ \left( \frac{dy\tilde{U}}{dy} \right)^2 + \frac{1}{2} \frac{d^2 y^2 \tilde{u}_{\text{rms}}^2}{dy^2} \right] + \langle \theta^2 \rangle (\tilde{w}_{\text{rms}}^2 - \tilde{u}_{\text{rms}}^2) + \dots, \quad (3.1)$$

$$v_{\text{rms}}^2(y) = \tilde{v}_{\text{rms}}^2(y) + \frac{1}{2} \langle u_{\tau_L}^{\prime 2} \rangle \frac{d^2 y^2 \tilde{v}_{\text{rms}}^2}{dy^2} + \dots, \quad (3.2)$$

$$w_{\text{rms}}^2(y) = \tilde{w}_{\text{rms}}^2(y) + \frac{1}{2} \langle u_{\tau_L}^{\prime 2} \rangle \frac{d^2 y^2 \tilde{w}_{\text{rms}}^2}{dy^2} + \langle \theta^2 \rangle (\tilde{U}^2 + \tilde{u}_{\text{rms}}^2 - \tilde{w}_{\text{rms}}^2) + \dots, \quad (3.3)$$

$$\langle u'v' \rangle(y) = \tilde{\tau}_R(y) + \frac{1}{2} \langle u_{\tau_L}^{\prime 2} \rangle \frac{d^2 y^2 \tilde{\tau}_R}{dy^2} - \frac{1}{2} \langle \theta^2 \rangle \tilde{\tau}_R + \dots, \quad (3.4)$$

where  $\tilde{u}_{\text{rms}}^2(\tilde{y}) = \left\langle \left( \tilde{u}(\tilde{y}) - \tilde{U}(\tilde{y}) \right)^2 \right\rangle$ ,  $\tilde{v}_{\text{rms}}^2(\tilde{y}) = \langle \tilde{v}^2 \rangle$ ,  $\tilde{w}_{\text{rms}}^2(\tilde{y}) = \langle \tilde{w}^2 \rangle$ , and the universal mean Reynolds stress  $\tilde{\tau}_R(\tilde{y}) = \left\langle \left( \tilde{u}(\tilde{y}) - \tilde{U}(\tilde{y}) \right) \tilde{v}(\tilde{y}) \right\rangle$ .

In the right-hand sides of (2.10) and (3.1-3.4) only  $\langle u_{\tau_L}^{\prime 2} \rangle$  and  $\langle \theta^2 \rangle$  vary with  $Re$ . In (2.10),  $\langle u_{\tau_L}^{\prime 2} \rangle$  and  $\langle \theta^2 \rangle$  are multiplied by a factor of the same order of magnitude as  $U(y)$  itself. Since variation of  $U(y)$  with  $Re$  is very small, the corresponding variation of  $\langle u_{\tau_L}^{\prime 2} \rangle$  and  $\langle \theta^2 \rangle$  should also to be small. Indeed, for  $Re_\tau$  in the range being considered (between 950 and 5200), the amplitude of large-scale motions is small. For example, for the filter used in (Zhang & Chernyshenko 2016),  $\langle u_{\tau_L}^{\prime 2} \rangle = 0.004364 = 4.364 \cdot 10^{-3}$  for  $Re = 1000$ , and for the filter used in (Zhang 2019)  $\langle u_{\tau_L}^{\prime 2} \rangle = 0.0031$  for  $Re_\tau = 950$  and  $\langle u_{\tau_L}^{\prime 2} \rangle = 0.0064$  for  $Re_\tau = 4200$ . This allows to conclude that  $\tilde{U}(y) \approx U(y)$ , and by the order of magnitude  $\tilde{u}_{\text{rms}}^2 \sim u_{\text{rms}}^2$ ,  $\tilde{v}_{\text{rms}}^2 \sim v_{\text{rms}}^2$ ,  $\tilde{w}_{\text{rms}}^2 \sim w_{\text{rms}}^2$ , and  $\tilde{\tau}_R \sim \langle u'v' \rangle(y)$ . Using this for estimating the terms in (2.10) and (3.1-3.4) shows that  $u_{\text{rms}}^2(y)$  and  $w_{\text{rms}}^2(y)$  stand out. In (3.1)  $\langle u_{\tau_L}^{\prime 2} \rangle$  is multiplied by  $(dy\tilde{U}/dy)^2$  and in (3.3)  $\langle \theta^2 \rangle$  is multiplied by  $\tilde{U}^2$ . These factors are large. At  $y^+ = 40$  for example,  $(dy\tilde{U}/dy)^2 \approx 285$ , which is almost 50 times greater than  $u_{\text{rms}}^2 \approx 6$ , and  $\tilde{U}^2 \approx 203$ , which is almost 85 times greater than  $w_{\text{rms}}^2 \approx 2.4$ . There are no such large terms in (2.10), (3.2), and (3.4). The term  $\langle u_{\tau_L}^{\prime 2} \rangle (dy\tilde{U}/dy)^2$  describes the combined

<sup>†</sup> We used the direct numerical simulations (DNS) of a plane channel flow data available at the turbulence.oden.utexas.edu file server and were obtained in the calculations described in (Hoyas & Jiménez 2006; Lee & Moser 2015). For the analysis, we fitted the velocity average and its nonzero second moments with explicit expressions. The fit is described in the Supplement.

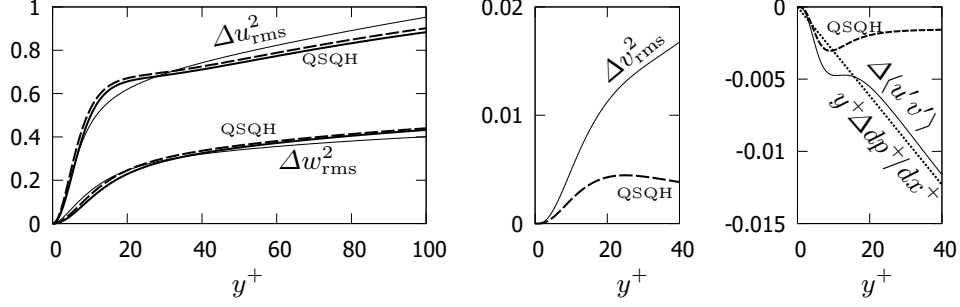


FIGURE 3. Comparison of the increments of the second moments as  $Re_\tau$  changes from 2000 to 5200. Thin curves are DNS results. The QSQH predictions are (3.9), shown with solid curves, and (3.5-3.8), shown with dashed curves. The dotted curve is  $y^+ \Delta p^+ / dx^+$ . The fit parameters are  $\Delta \langle \theta^2 \rangle = 0.0016$  and  $\Delta \langle u_{\tau L}^{\prime 2} \rangle = 0.0025$ .

action of the amplitude modulation and modulation of the wall-normal length scale of the universal mean profile, which is a QSQH mechanism described in (Chernyshenko *et al.* 2012; Zhang & Chernyshenko 2016). The term  $\langle \theta^2 \rangle \tilde{U}^2$  describes the turning of the universal mean profile to follow the fluctuating direction of the large-scale wall friction. Such large terms are not present in the expressions for other quantities. This explains why  $u_{\text{rms}}^2$  and  $w_{\text{rms}}^2$  vary more with  $Re$  than  $U$ ,  $v_{\text{rms}}^2$  and  $\langle u'v' \rangle$ .

### 3.2. The profiles of the change in the second moments with $Re$

The precise values of  $\langle u_{\tau L}^{\prime 2} \rangle$  and  $\langle \theta^2 \rangle$  and the statistics of the universal velocity depend on the definition of the large-scale filter. Luckily, since  $\langle u_{\tau L}^{\prime 2} \rangle$  and  $\langle \theta^2 \rangle$  are small,  $\tilde{U}$  is known quite accurately, and the second moments can be estimated approximately by taking  $\tilde{u}_{\text{rms}}^2 \approx u_{\text{rms}}^2$ ,  $\tilde{v}_{\text{rms}}^2 \approx v_{\text{rms}}^2$ ,  $\tilde{w}_{\text{rms}}^2 \approx w_{\text{rms}}^2$ , and  $\tilde{\tau}_R \approx \langle u'v' \rangle$ . Moreover, the dominance of the terms  $\langle \theta^2 \rangle \tilde{U}^2$  and  $\langle u_{\tau L}^{\prime 2} \rangle (dy\tilde{U}/dy)^2$  allows to express the shape of the increase in  $u_{\text{rms}}^2$  and  $w_{\text{rms}}^2$  with  $Re$  as a function of the wall distance in terms of the shape of the mean velocity profile only.

Using (3.1-3.4), the increments of the second order moments between two values of  $Re$  can be expressed in terms of the increments of  $\langle u_{\tau L}^{\prime 2} \rangle$  and  $\langle \theta^2 \rangle$  as

$$\Delta u_{\text{rms}}^2 = \Delta \langle u_{\tau L}^{\prime 2} \rangle \left[ \left( \frac{dy\tilde{U}}{dy} \right)^2 + \frac{1}{2} \frac{d^2 y^2 \tilde{u}_{\text{rms}}^2}{dy^2} \right] + \Delta \langle \theta^2 \rangle (\tilde{w}_{\text{rms}}^2 - \tilde{u}_{\text{rms}}^2) + \dots, \quad (3.5)$$

$$\Delta v_{\text{rms}}^2 = \frac{\Delta \langle u_{\tau L}^{\prime 2} \rangle}{2} \frac{d^2 y^2 \tilde{v}_{\text{rms}}^2}{dy^2} + \dots, \quad (3.6)$$

$$\Delta w_{\text{rms}}^2 = \frac{\Delta \langle u_{\tau L}^{\prime 2} \rangle}{2} \frac{d^2 y^2 \tilde{w}_{\text{rms}}^2}{dy^2} + \Delta \langle \theta^2 \rangle (\tilde{U}^2 + \tilde{u}_{\text{rms}}^2 - \tilde{w}_{\text{rms}}^2) + \dots, \quad (3.7)$$

$$\Delta \langle u'v' \rangle = \frac{\Delta \langle u_{\tau L}^{\prime 2} \rangle}{2} \frac{d^2 y^2 \tilde{\tau}_R}{dy^2} - \frac{1}{2} \langle \theta^2 \rangle \tilde{\tau}_R + \dots, \quad (3.8)$$

If the terms we identified to be small are dropped, this becomes

$$\Delta u_{\text{rms}}^2 \approx \Delta \langle u_{\tau L}^{\prime 2} \rangle \left( \frac{dy\tilde{U}}{dy} \right)^2, \quad \Delta w_{\text{rms}}^2 \approx \Delta \langle \theta^2 \rangle \tilde{U}^2, \quad \Delta v_{\text{rms}}^2 \approx \Delta \langle u'v' \rangle \approx 0. \quad (3.9)$$

Without the filter being specified,  $\Delta \langle u_{\tau L}^{\prime 2} \rangle$  and  $\Delta \langle \theta^2 \rangle$  remain unknown. It is still

possible to compare if not the magnitude but at least the shape of the curves of  $\Delta u_{\text{rms}}^2(y)$  and  $\Delta w_{\text{rms}}^2(y)$  with the QSQH prediction (3.9). For  $Re_\tau$  changing from 2000 to 5200 this prediction is shown in figure 3 with thick solid lines. For illustrative purpose we chose the values  $\Delta\langle\theta^2\rangle = 0.0016$  and  $\Delta\langle u_{\tau_L}^{\prime 2}\rangle = 0.0025$  †. (An alternative is to take a logarithmic derivative as in figure 12 of (Zhang & Chernyshenko 2016), but this would not apply for other formulae here.) Overall, the deviation of the QSQH predictions for  $\Delta u_{\text{rms}}^2$  and  $\Delta w_{\text{rms}}^2$  is not large and is of the same order of magnitude as reported in most cases in (Zhang & Chernyshenko 2016). This further confirms that near the wall the variation of  $u_{\text{rms}}^2$  and  $w_{\text{rms}}^2$  with  $Re$  is dominated by the QSQH mechanism.

The values  $\Delta\langle\theta^2\rangle = 0.0016$  and  $\Delta\langle u_{\tau_L}^{\prime 2}\rangle = 0.0025$  can also be used in (3.6-3.8). Predictions obtained with these values are shown in figure 3 with dashed lines. The small difference between the QSQH predictions for  $\Delta u_{\text{rms}}^2$  and  $\Delta w_{\text{rms}}^2$  obtained using (3.9) and (3.5,3.7) confirms that the terms dropped in (3.9) are small.

The QSQH predictions for  $\Delta v_{\text{rms}}^2$  and  $\Delta\langle u'v'\rangle$  deviate considerably, by an order of magnitude, from the DNS results. The almost linear behaviour of  $\Delta\langle u'v'\rangle$  for  $y^+ > 20$  suggests an explanation. It is well-known that the dependence of the total shear stress on the distance to the channel wall is linear and in wall units is equal to  $y^+ dp^+/dx^+ = y^+/Re_\tau$ , and that further away from the wall the Reynolds stress approaches the total stress. As  $Re_\tau$  changes, so does the pressure gradient. The corresponding change in the total stress, equal to  $\Delta y^+ dp/dx = y^+(1/5200 - 1/2000)$ , is shown with a dotted line in figure 2 and fits the deviation between the QSQH prediction and DNS. Therefore, the deviation is due to the QSQH theory not taking into account the nonzero pressure gradient in a channel flow.

#### 4. The effect of the fluctuations of the direction of large-scale skin friction on the conditional averages of spanwise velocity

For the channel flow at  $Re_\tau = 1000$ , Agostini & Leschziner (2019b) plotted (in different notation) the conditional average  $\hat{w}^2(\hat{y}, u_{\tau_L x}) = \left\langle (w(yu_{\tau_L x})/u_{\tau_L x})^2 \right\rangle_{u_{\tau_L x}}$  versus  $\hat{y} = yu_{\tau_L x}$  for several values of  $u_{\tau_L x} = u_{\tau_L} \cos\theta$ . Unlike other parameters, the curves of  $\hat{w}^2(\hat{y}, u_{\tau_L x})$  for different values of  $u_{\tau_L x}$  deviated from each other to a certain degree even quite close to the wall. If the fluctuations of the direction of the large-scale component of skin friction were negligible (that is if  $\theta = 0$ ),  $\hat{w}^2$  would coincide with  $\tilde{w}^2$ , and according the QSQH assumption, the curves should be independent of  $u_{\tau_L}$ . There are three possible reasons for the deviation: neglecting the fluctuations of the large-scale component of the wall friction, the imperfection of the large-scale filter used, and the approximate nature of the QSQH hypothesis. We will consider first how taking into account that  $\theta \neq 0$  affects this issue. Agostini & Leschziner (2019b) mentioned that using for scaling the large-scale friction velocity  $u_{\tau_L}$  instead of its  $x$ -component does not make much difference. Conditionally averaging the square of (2.9) for fixed  $u_{\tau_L}$  and using the filter properties and symmetry gives

$$\left\langle \frac{w^2}{u_{\tau_L}^2} \right\rangle_{u_{\tau_L}} = \left( \tilde{U}^2(\tilde{y}) + \tilde{u}_{\text{rms}}^2(\tilde{y}) - \tilde{w}_{\text{rms}}^2(\tilde{y}) \right) \langle \sin^2 \Theta \rangle_{u_{\tau_L}} + \tilde{w}_{\text{rms}}^2(\tilde{y}). \quad (4.1)$$

† The comparisons of the increments as  $Re_\tau$  changes from 950 to 2000 and from 1000 to 2000, not shown here, gave similar results. By coincidence, the same values of  $\Delta\langle\theta^2\rangle$  and  $\Delta\langle u_{\tau_L}^{\prime 2}\rangle$  roughly fit also the 950 to 2000 case.

Therefore,  $\langle w^2/u_{\tau_L}^2 \rangle|_{u_{\tau_L}}$  varies with  $u_{\tau_L}$  in proportion to the variation of  $\langle \sin^2 \Theta \rangle|_{u_{\tau_L}}$ . Since  $\tilde{U}^2$  is greater than the other terms, (4.1) implies that the increment of  $\langle w^2/u_{\tau_L}^2 \rangle|_{u_{\tau_L}}$  as  $u_{\tau_L}$  varies has the same sign for all values of  $\tilde{y}$ . However, the shape of the curves of  $\langle w^2/u_{\tau_L}^2 \rangle|_{u_{\tau_L}}$  in figure 4(f) in (Agostini & Leschziner 2019b) shows that in fact this increment changes the sign at approximately  $\tilde{y} = 70$ . Hence, if the QSQH theory were expected to be valid for  $\tilde{y} \approx y^+ > 70$ , accounting for the fluctuation of the direction of the large-scale wall friction would not explain the discrepancy. For  $\tilde{y} < 70$  taking into account the fluctuations of the large-scale friction direction might improve the collapse of the curves of  $\langle w^2/u_{\tau_L}^2 \rangle|_{u_{\tau_L}}$  provided that  $\langle \sin^2 \Theta \rangle|_{u_{\tau_L}}$  suitably increases with  $u_{\tau_L}$ .

The deviation from the QSQH theory might also be caused by the properties of the bi-dimensional EMD filter used in (Agostini & Leschziner 2019b). Indeed, the EMD filter does not satisfy properties (i), (iii), and (iv) of the QSQH filter. This, for example, invalidates the application of (4.1) to the results of (Agostini & Leschziner 2019b). On the other hand, the EMD filter can be expected to satisfy to a reasonable degree the property (v), since both the EMD and the conventional Fourier cut-off filter were found to be effective in separating the scales (Dogan *et al.* 2018). A deeper analysis is complicated for the following reasons. The large-scale motions and the small-scale motions obtained using the bi-dimensional EMD filter are not guaranteed to satisfy continuity. Hence, there is an exchange of mass, momentum and energy between the large and small scales thus defined. Also, the small-scale motions defined using the EMD filter are not guaranteed to have zero average and appear to actually have a nonzero average (see figure 1(b) in (Agostini & Leschziner 2019b)). As a result, even an intuitive reasoning about the results obtained using this filter is hard. We have to postpone further judgment until a thorough analysis of the above features of the bi-dimensional EMD filter becomes available.

It remains to consider the third explanation, namely, that the observed behaviour of  $\hat{w}^2(\hat{y}, u_{\tau_L, x})$  is caused by the approximate nature of the QSQH theory.

## 5. Approximate nature and applications of the QSQH theory

Approximate theories are ubiquitous. Their validity is often judged by comparing their predictions with known answers. Note that for any approximate theory it is easy to construct a comparison giving an arbitrary large relative error. Let  $y(x)$  be the unknown. Let the exact but unknown formula for it be  $y = f(x)$ , and let the approximate formula be  $y = f_a(x)$ . Consider another unknown,  $z(x)$ , defined as  $z = y - f_a(x)$ . For this second unknown the approximate theory gives the answer  $z = 0$ , the relative error of which is infinity. When numerous comparisons are made, a situation close to this artificial construction can occur by chance. For this reason, approximate theories should be judged by what they can predict rather than by what they cannot predict.

The comparisons in Section 3 clearly illustrate this point. Within the range of wall distances and Reynolds numbers we considered, the pressure gradient is a much weaker effect than the quasi-steady-quasi-homogeneous modulation of the near-wall turbulence by the large-scale structures. To see this one needs only to compare the scales of the three plots in figure 3. However, if the fidelity of the QSQH theory was judged by the comparisons for the variation of  $\langle u'v' \rangle$ , it could be erroneously rejected.

There are flow features that the QSQH theory does not predict by its very nature. Assuming that the universal velocity is statistically homogeneous in the wall-parallel directions and that it satisfies continuity and impermeability condition at the wall gives that the mean wall-normal universal velocity  $\tilde{V} = 0$ . Then, applying the large-scale filter to (2.4), noticing that  $v = v_\theta$ , and using the filter properties gives that the large-scale

component of the wall-normal velocity is zero:  $v_L = u_{\tau_L} \tilde{V} = 0$ . Within the QSQH theory, this is consistent. The theory is based on the assumption that the large scales are much larger than the small scales, and thus it effectively neglects the derivatives of large-scale components in wall-parallel directions. Then from continuity and impermeability condition it indeed follows that  $v_L = 0$ . On the other hand, in reality the wall-normal component of the velocity of the large-scale motions is nonzero. Another flow feature not accounted for by the QSQH theory is the three-dimensional structure of the large-scale motions. The large-scale motions enter the QSQH theory only through the wall friction, which is independent of wall-normal distance by definition. This list can be continued.

There are interesting questions concerning the QSQH hypothesis. Will its error tend to zero as  $Re \rightarrow \infty$  in spite of the smallest of the large scales remaining close to the largest of the small scales? Does the range of the distances from the wall where the QSQH theory applies extend as  $Re$  increases? At moderate  $Re$  the fluctuations of the large-scale motions are small on average, but there are rare large deviations. Is the QSQH theory applicable to these rare events? Answering these questions requires further studies.

The similarity between the classical universality hypothesis and the QSQH hypothesis suggests that these hypotheses should be used similarly. The classical hypothesis describes a well-known dominant feature of near-wall turbulent flows. This feature can obscure other physics, unless the wall units are used. Similarly, the QSQH hypothesis describes a dominant feature of the effect of large-scale motions on the near-wall turbulence. Similarly, the QSQH mechanisms can obscure other mechanisms, unless the appropriate QSQH units, corresponding to the ‘tilde’ variables  $\tilde{t}, \tilde{x}, \tilde{y}, \tilde{z}, \tilde{u}, \tilde{v}, \tilde{w}$ , introduced by (2.3-2.6), are used. For this reason, the use of these variables is preferable in studies of the effect of large-scale motion on near-wall turbulence. A very welcome step towards using the QSQH variables is the study by Agostini & Leschziner (2019b), a part of which we discussed in Section 4. Even though this work did not account for the fluctuation of the direction of the wall friction, it provided extensive direct evidence that using the QSQH variables leads to a better collapse of data than the use of variables in wall units. It is also the first work where the QSQH variables are used for studying non-QSQH effects.

## 6. Conclusions

The extension of the QSQH theory proposed in the present paper takes into account the fluctuations of the large-scale component of the wall friction. It describes the effect of large-scale motions on all three components of the velocity of near-wall turbulent flows. The extended theory explains the large sensitivity of the magnitudes  $u_{\text{rms}}$  and  $w_{\text{rms}}$  of the fluctuations of longitudinal and spanwise velocities to Reynolds number in comparison with the sensitivity of the mean velocity profile, the Reynolds stress, and the magnitude of the fluctuations of the wall-normal velocity. It is shown that the variation of  $u_{\text{rms}}$  with  $Re$  is largely caused by the variation of the amplitude and wall-normal-scale modulation by the outer, large-scale,  $Re$ -dependent motions, while the variation of  $w_{\text{rms}}$  is largely caused by the fluctuations of the direction of the large-scale,  $Re$ -dependent, component of the wall friction. The  $Re$  dependence of the other second moments is not dominated by these mechanisms because the mean universal wall-normal velocity is zero. In particular, the effect of the variation of the mean pressure gradient with  $Re$  is stronger than the QSQH mechanisms as far as the variation of the Reynolds stress with  $Re$  is concerned. The analysis of the quality of the QSQH approximate nature suggests that it is beneficial to use the units and variables of the QSQH theory instead of the wall units in studies of flows where the effect of large-scale motions on the near-wall turbulence is relevant.

Declaration of Interests. The author reports no conflict of interest.

## REFERENCES

- AGOSTINI, L. & LESCHZINER, M. 2018 The impact of footprints of large-scale outer structures on the near-wall layer in the presence of drag-reducing spanwise wall motion. *Flow, Turbulence and Combustion* **100** (4), 1037–1061.
- AGOSTINI, L. & LESCHZINER, M. 2019a The connection between the spectrum of turbulent scales and the skin-friction statistics in channel flow at  $Re_\tau \approx 1000$ . *J. Fluid Mech.* **871**, 22–51.
- AGOSTINI, L. & LESCHZINER, M. 2019b On the departure of near-wall turbulence from the quasi-steady state. *J. Fluid Mech.* **871**, R1.
- AGOSTINI, L., LESCHZINER, M., POGGIE, J., BISEK, N. J. & GAITONDE, D. 2017 Multi-scale interactions in a compressible boundary layer. *J. Turb.* **18** (8), 760–780.
- AGOSTINI, L. & LESCHZINER, M. A. 2014 On the influence of outer large-scale structures on near-wall turbulence in channel flow. *Phys. Fluids* **26**.
- BAARS, W., HUTCHINS, N. & MARUSIC, I. 2017 Reynolds number trend of hierarchies and scale interactions in turbulent boundary layers. *Phil. Trans. R. Soc. Lond.* **375**, 20160077.
- BAARS, W. J., HUTCHINS, N. & MARUSIC, I. 2016 Spectral stochastic estimation of high-Reynolds-number wall-bounded turbulence for a refined inner-outer interaction model. *Phys. Rev. Fluids* **1**, 054406.
- CHERNYSHENKO, S. I., MARUSIC, I. & MATHIS, R. 2012 Quasi-steady description of modulation effects in wall turbulence, arXiv: arXiv:1203.3714.
- CHERNYSHENKO, S. I., ZHANG, C., BUTT, H. & BEIT-SADI, M. 2019 A large-scale filter for applications of QSQH theory of scale interactions in near-wall turbulence. *Fluid Dyn. Res.* **51** (1), 011406.
- DOGAN, E., ÖRLÜ, R., GATTI, D., VINUESA, R. & SCHLATTER, P. 2018 Revisiting the amplitude modulation in wall-bounded turbulence: towards a robust definition, arXiv: 1812.03683.
- GANAPATHISUBRAMANI, B., HUTCHINS, N., MONTY, J.P., CHUNG, D. & MARUSIC, I. 2012 Amplitude and frequency modulation effects in wall turbulence. *J. Fluid Mech.* **712**, 61–91.
- HOWLAND, M. F. & YANG, X. I. A. 2018 Dependence of small-scale energetics on large scales in turbulent flows. *J. Fluid Mech.* **852**, 641–662.
- HOYAS, S. & JIMÉNEZ, J. 2006 Scaling of the velocity fluctuations in turbulent channels up to  $Re_\tau = 2003$ . *Phys. Fluids* **18** (011702), 1–4.
- HUTCHINS, N. & MARUSIC, I. 2007 Large-scale influences in near-wall turbulence. *Phil. Trans. R. Soc. Lond.* **365**, 647–664.
- LEE, M. & MOSER, R. D. 2015 Direct numerical simulation of turbulent channel flow up to  $Re_\tau=5200$ . *J. Fluid Mech.* **774**, 395–415.
- LOZIER, M., MIDYA, S., THOMAS, F. O. & GORDEYEV, S. 2019 Experimental studies of boundary layer dynamics using active flow control of large-scale structures. In *11th International Symposium on Turbulence and Shear Flow Phenomena (TSFP11)*. Southampton, UK.
- MARUSIC, I., MATHIS, R. & HUTCHINS, N. 2010 Predictive model for wall-bounded turbulent flow. *Science* **329** (5988), 193–196.
- MATHIS, R., HUTCHINS, N. & MARUSIC, I. 2009 Large-scale amplitude modulation of the small-scale structures in turbulent boundary layers. *J. Fluid Mech.* **628**, 311–337.
- RAO, K.N., NARASIMHA, R. & NARAYANAN, M.A.B. 1971 The “bursting” phenomenon in a turbulent boundary layer. *J. Fluid Mech.* **48**, 339–352.
- SMITS, A. J., MCKEON, B. J. & MARUSIC, I. 2011 High-Reynolds number wall turbulence. *Annu. Rev. Fluid Mech.* **43**, 353–375.
- ZHANG, C. 2019 Quasi-steady quasi-homogenous (QSQH) theory of the relationship between large-scale and small-scale motions in near-wall turbulence. PhD thesis, Imperial College London, supervisors Chernyshenko, S. and Leschziner, M.
- ZHANG, C. & CHERNYSHENKO, S. I. 2016 Quasisteady quasihomogeneous description of the scale interactions in near-wall turbulence. *Phys. Rev. Fluids* **1**, 014401.

**Analytic fits for the mean velocity and second moments of velocity near the wall for a turbulent flow in a plane channel: a supplement for the paper “Extension of QSQH theory of scale interaction in near-wall turbulence to all velocity components”**

Sergei Chernyshenko

Department of Aeronautics, Imperial College London

s.chernyshenko@imperial.ac.uk

When making comparisons it is sometimes convenient to use analytic fits to the results of direct numerical simulations, even if only for plotting. Analytic expressions can also be differentiated, even though this involves a certain loss of accuracy. The analytic expressions were obtained by fitting the direct numerical simulation data for a plane channel flow with  $Re_\tau = 180, 550, 950, 1000, 2000, 5200$ . The DNS data were downloaded from the turbulence.oden.utexas.edu file server. The calculations are by Hoyas, S. & Jiménez [1] and Lee & Moser [2]. Fitting was done over the range of  $0 \leq y^+ \leq 100$  using gnuplot command ‘fit’.

The profiles are expressed via the following functions and their powers:

$$f(y, a, b, c, q, r, p) = y(ay^2 + by + c)/(qy^2 + ry + 1) + p \log(y + 1)$$

and

$$f_{15}(y, a, b, c, q, r, p) = y(ay^2 + by + c)/(qy^2 + ry + 1) + p(\log(y + 15) - \log(15)),$$

$\log$  is a natural logarithm, and  $a, b, c, q, r, p$  are the fitting parameters. These expressions in the text form suitable for cutting and pasting into a code are:

$$\begin{aligned} f(x,a,b,c,q,r,p) &= x*(a*x**2 + b*x+c)/(q*x**2+r*x+1)+p*log(x+1) \\ f15(x,a,b,c,q,r,p) &= x*(a*x**2 + b*x+c)/(q*x**2+r*x+1)+p*(log(x+15)-log(15)) \end{aligned}$$

The mean velocity  $U^+(y^+)$ , the root mean squares  $u_{\text{rms}} = \sqrt{\langle u'u' \rangle}$ ,  $v_{\text{rms}} = \sqrt{\langle v'v' \rangle}$ ,  $w_{\text{rms}} = \sqrt{\langle w'w' \rangle}$ , and the Reynolds stress  $\langle u'v' \rangle$  were fitted. All the variables are in wall units. The following pages give the representation of the fitted quantities in terms of  $f$  and/or  $f_{15}$ , plots with comparisons with DNS, and expressions in the text form suitable for cutting and pasting into a code. A text file with all these expressions is provided separately. The notation is intended to be self-explanatory. LM stands for Lee & Moser and HJ is for Hoyas & Jiménez, Re is  $Re_\tau$  based on the channel half-width.

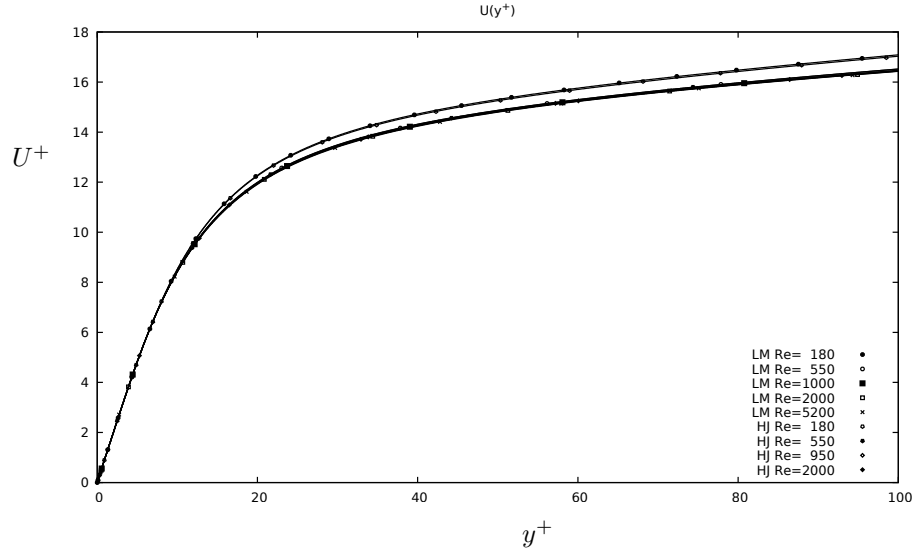


Figure 1: Mean velocity

$$U(y) = f(y, a, b, c, q, r, p) = y(ay^2 + by + c)/(qy^2 + ry + 1) + p \log(y + 1)$$

URe5200LM(x)=f(x,0.000155064859152652,0.124332316558984, 0.585852700238061,0.00960750534540338,0.0589324149643223, 0.493534445516441)  
 URe2000LM(x)=f(x,0.000154587935701633,0.121945362785562, 0.608802562811952,0.00934699868156456,0.058394426829014, 0.461629411942626)  
 URe1000LM(x)=f(x,0.000155568705758487,0.118289838303881, 0.619767033981213,0.00906452697385482,0.0562936331642849, 0.448968282677922)  
 URe0550LM(x)=f(x,0.000159454562845575,0.113267163433361, 0.636816719993512,0.0086861909085036, 0.0537966403282146, 0.428997666967737)  
 URe0180LM(x)=f(x,0.000164300321807816,0.0961432399193651,0.665040474947198,0.00728557305508607,0.044548055977009, 0.403728726538813)  
 URe2000HJ(x)=f(x,0.000155003439789658,0.121889353641462, 0.59668758158729, 0.00939945611981467,0.0576292141831145,0.480987959245497)  
 URe0950HJ(x)=f(x,0.000154946383447842,0.118568062133334, 0.613795545234793,0.00911155818726103,0.0561254847028229,0.457504875767387)  
 URe0550HJ(x)=f(x,0.000159480212600236,0.115284348323668, 0.619866802062511,0.00887866344547915,0.0541168724687089,0.451237458085645)  
 URe0180HJ(x)=f(x,0.000166302434061266,0.0963047516739797,0.65762882934244, 0.00736574280029303,0.0438959832544501,0.414636835720395)

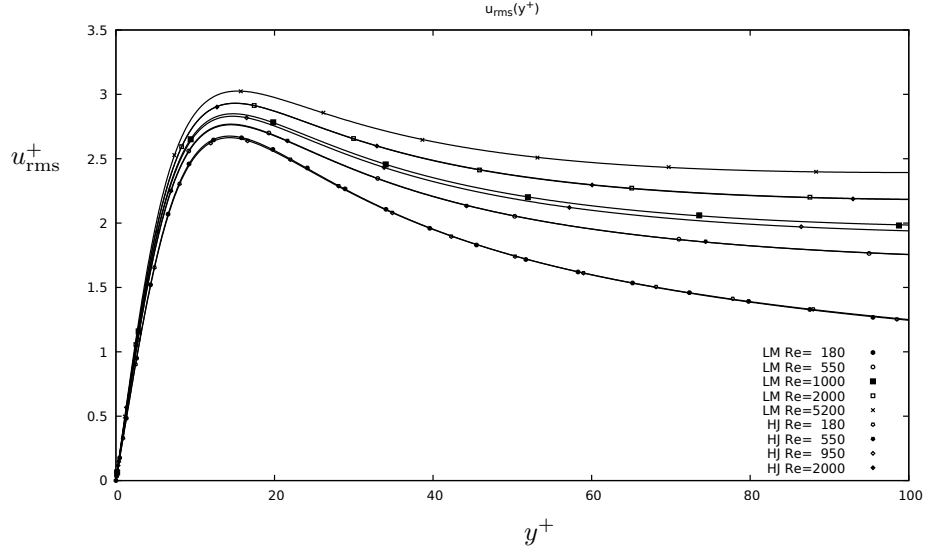


Figure 2:  $u_{\text{rms}}$

$$u_{\text{rms}}(y) = f_{15}(y, a, b, c, q, r, p) = y(ay^2 + by + c) / (qy^2 + ry + 1) + p(\log(y+15) - \log(15))$$

$u_{\text{rms}}\text{Re}0180\text{LM}(x) = f_{15}(x, -2.96511771502127e-06, 0.00713098516423203, 0.368618519092697, 0.00724292079273704, -0.00188104534382705, -0.0939004345943289)$   
 $u_{\text{rms}}\text{Re}0550\text{LM}(x) = f_{15}(x, 2.58534223375324e-05, 0.0122455777205154, 0.404018861588927, 0.00889216822122883, 0.00606957761017823, -0.161778516477361)$   
 $u_{\text{rms}}\text{Re}1000\text{LM}(x) = f_{15}(x, 2.78859635192058e-05, 0.0128912190206297, 0.411914517490417, 0.00914911302483312, 0.0072420062970093, -0.0682978880267656)$   
 $u_{\text{rms}}\text{Re}2000\text{LM}(x) = f_{15}(x, 2.623240525666284e-05, 0.0134321561634876, 0.418549175660149, 0.0093889429802691, 0.00778354559725009, 0.0338138600827896)$   
 $u_{\text{rms}}\text{Re}5200\text{LM}(x) = f_{15}(x, 2.42123399342968e-05, 0.0137260007931729, 0.42570940965966, 0.00952531539247033, 0.00816310356056566, 0.142743764676396)$   
 $u_{\text{rms}}\text{Re}0180\text{HJ}(x) = f_{15}(x, -2.0232289518942e-06, 0.00733887166563185, 0.367270461585974, 0.007282396904903, -0.00154082404494924, -0.106440998116575)$   
 $u_{\text{rms}}\text{Re}0550\text{HJ}(x) = f_{15}(x, 2.60422226343772e-05, 0.0121332976235026, 0.402982812604456, 0.00885549199322238, 0.00613798778956479, -0.159540875042328)$   
 $u_{\text{rms}}\text{Re}0950\text{HJ}(x) = f_{15}(x, 2.4616787538755e-05, 0.012502990497006, 0.40893942174543, 0.00910233275841391, 0.00663208739941688, -0.0569507277015093)$   
 $u_{\text{rms}}\text{Re}2000\text{HJ}(x) = f_{15}(x, 2.66287209386734e-05, 0.0133615203710217, 0.418719266671255, 0.00937082552090975, 0.00775475024639174, 0.0324648258779921)$

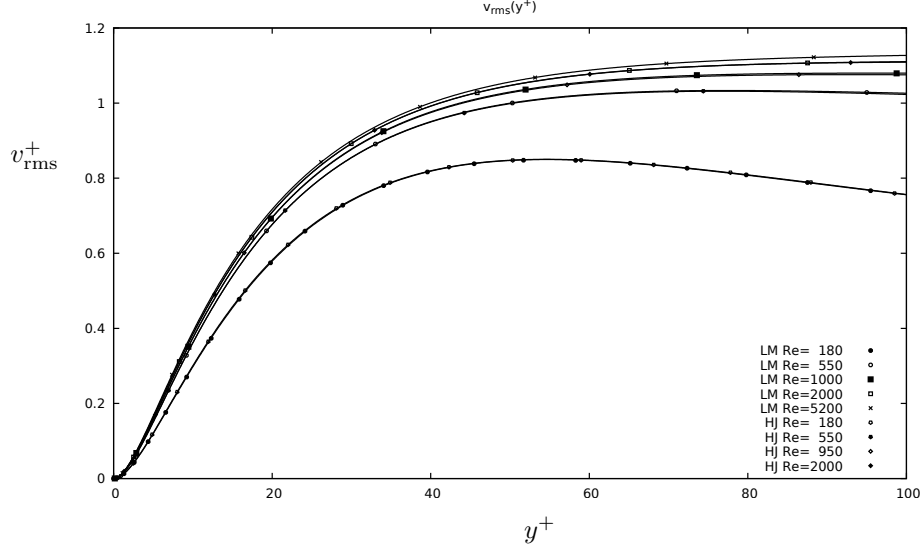


Figure 3:  $v_{\text{rms}}$

$$v_{\text{rms}}(y) = f_{15}^2(y, a, b, c, q, r, p) = (y(ay^2 + by + c)/(qy^2 + ry + 1) + p(\log(y + 15) - \log(15)))^2$$

```

vsqrtrmsRe0180LM(x)=f15(x, 2.41938530630219e-06, -0.005892068856212848, -0.0077676262782838, 0.000828781770821384, 0.154590693259966, 1.56314045596651)
vsqrtrmsRe0550LM(x)=f15(x, -3.62370968972199e-06, -0.00771444345752978, -0.0132743698870516, 0.0013922374768463, 0.147054321405927, 1.85771815751584)
vsqrtrmsRe1000LM(x)=f15(x, -4.1893276442043e-06, -0.00799556103055885, -0.0117451244065584, 0.00146866281868965, 0.147654082043006, 1.8856633345211)
vsqrtrmsRe2000LM(x)=f15(x, -4.63204035488413e-06, -0.00823521098799527, -0.00900585799466542, 0.00153937507562706, 0.149967447907337, 1.8918597191896)
vsqrtrmsRe5200LM(x)=f15(x, -5.54815570335504e-06, -0.0091658705452141, -0.0115209267452397, 0.00167001292415056, 0.157343089533074, 1.96548649536376)
vrmsRe0180LM(x)=vsqrtrmsRe0180LM(x)**2
vrmsRe0550LM(x)=vsqrtrmsRe0550LM(x)**2
vrmsRe1000LM(x)=vsqrtrmsRe1000LM(x)**2
vrmsRe2000LM(x)=vsqrtrmsRe2000LM(x)**2
vrmsRe5200LM(x)=vsqrtrmsRe5200LM(x)**2
vsqrtrmsRe0180HJ(x)=f15(x, 9.65439923792012e-07, -0.00709909883501314, -0.0127371958888107, 0.00105054100367451, 0.169102448901133, 1.65886763757801)
vsqrtrmsRe0550HJ(x)=f15(x, -4.78060080164494e-06, -0.00864264739332554, -0.0176231572361471, 0.00152284981682245, 0.155121745948214, 1.93455363238752)
vsqrtrmsRe0950HJ(x)=f15(x, -4.46099073773041e-06, -0.00816966657663943, -0.0123845666354246, 0.0014956398243829, 0.149357021643905, 1.89801856396605)
vsqrtrmsRe2000HJ(x)=f15(x, -1.21797163605269e-05, -0.0157105582660346, -0.0416069555393806, 0.0023632813495, 0.202766339807415, 2.41307665699363)
vrmsRe2000HJ(x)=vsqrtrmsRe2000HJ(x)**2
vrmsRe0950HJ(x)=vsqrtrmsRe0950HJ(x)**2
vrmsRe0550HJ(x)=vsqrtrmsRe0550HJ(x)**2
vrmsRe0180HJ(x)=vsqrtrmsRe0180HJ(x)**2

```

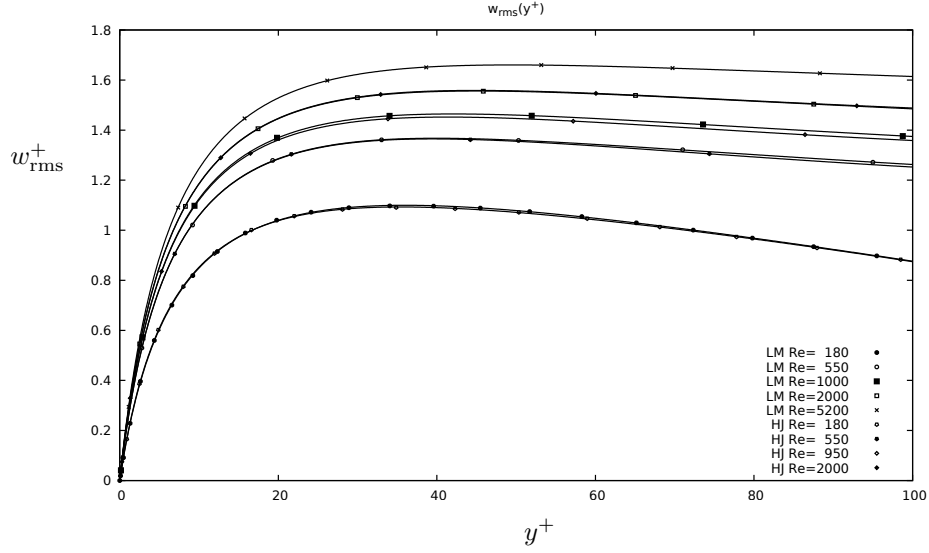


Figure 4:  $w_{\text{rms}}$

$$w_{\text{rms}}(y) = f_{15}(y, a, b, c, q, r, p) = y(ay^2 + by + c) / (qy^2 + rx + 1) + p(\log(y+15) - \log(15))$$

$w_{\text{rmsRe0180LM}}(x) = f_{15}(x, -2.04534705125964e-05, -0.00638020344624595, 0.121205632571833, 0.00231725044396721, 0.16939693949413, 1.29171921662097)$   
 $w_{\text{rmsRe0550LM}}(x) = f_{15}(x, -5.85344373638104e-06, -0.00789945389929343, 0.173618817273645, 0.00204585414584547, 0.179950441311365, 1.45966054095059)$   
 $w_{\text{rmsRe1000LM}}(x) = f_{15}(x, -5.90837356791285e-06, -0.00743709757663359, 0.190362109612082, 0.00204567529079099, 0.176653687437557, 1.44339839948606)$   
 $w_{\text{rmsRe2000LM}}(x) = f_{15}(x, -6.70256935487831e-06, -0.00725894289215538, 0.200140297679313, 0.00208929203393882, 0.172450786312379, 1.4726031977162)$   
 $w_{\text{rmsRe5200LM}}(x) = f_{15}(x, -8.94631764983125e-06, -0.0084598574019162, 0.191311317447557, 0.00218061920820277, 0.166057798726084, 1.71943819382951)$   
 $w_{\text{rmsRe0180HJ}}(x) = f_{15}(x, -4.0412927558585e-05, -0.0170065932647172, 0.0495404717376413, 0.00304789096947113, 0.189338120863009, 2.43086522096585)$   
 $w_{\text{rmsRe0550HJ}}(x) = f_{15}(x, 3.32805132121153e-05, 0.0272744795173471, 0.365649546944411, 0.0062019719528945, 0.198186594343618, -1.41550156068556)$   
 $w_{\text{rmsRe0950HJ}}(x) = f_{15}(x, 3.20298512131681e-05, 0.0265164208411655, 0.372681804636301, 0.0062630619696859, 0.195930883247131, -1.30612633893608)$   
 $w_{\text{rmsRe2000HJ}}(x) = f_{15}(x, 3.10318707015377e-05, 0.0273777055381056, 0.371979111530335, 0.00702168956398879, 0.19985554051313, -1.11038827797596)$

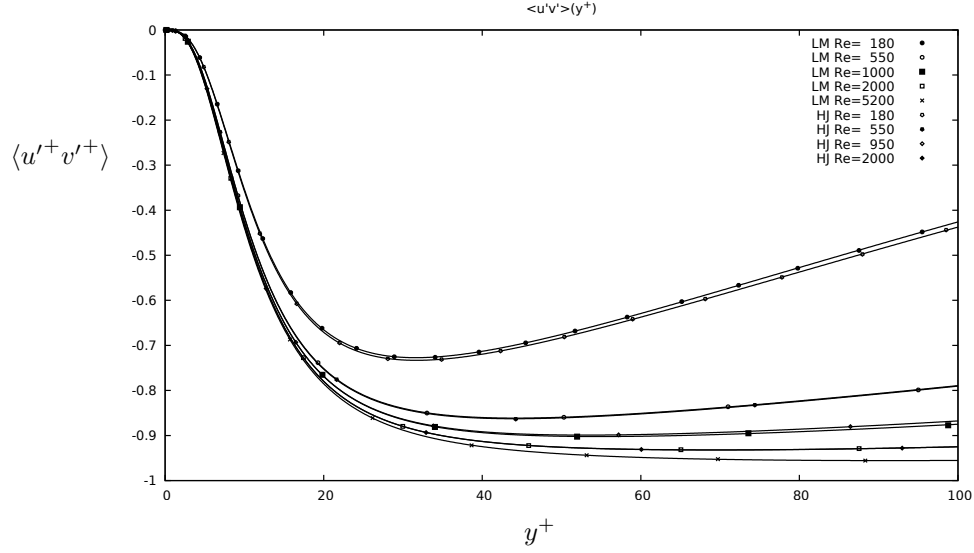


Figure 5: Reynolds stress

$$\langle u'v' \rangle(y) = -f_{15}^3(y, a, b, c, q, r, p) = -(y(ay^2 + by + c)/(qy^2 + ry + 1) + p(\log(y + 15) - \log(15)))^3$$

```

uvmeanonethridRe5200LM(x)=-f15(x,-6.00235084251445e-06,0.0110393880134619,0.0971494514578099,0.0130740607504558,0.0560872281771557,0.0756599507715887)
uvmeanonethridRe2000LM(x)=-f15(x,-7.84036407745564e-06,0.0104994462335006,0.0954735210603693,0.0126525035622012,0.0529466282944463,0.0839618555498294)
uvmeanonethridRe1000LM(x)=-f15(x,-1.1095556379209e-05,0.00992872527830186,0.0930050150094885,0.0122329354646834,0.0494819001584414,0.0964466884083661)
uvmeanonethridRe0550LM(x)=-f15(x,-1.59595147229951e-05,0.0093134863610134,0.0903362030849532,0.0117460658495685,0.0462169807046629,0.109839166662012)
uvmeanonethridRe0180LM(x)=-f15(x,-4.21477317909565e-05,0.00628540745070078,0.0746623203329355,0.00944055500852679,0.0314695416519397,0.229052223299449)
uvmeanonethridRe2000HJ(x)=-f15(x,-7.98298357378521e-06,0.0105404260114485,0.0953981402353763,0.0126992843177695,0.0529534563160199,0.0843797100585562)
uvmeanonethridRe0950HJ(x)=-f15(x,-1.14314892385872e-05,0.00993283249037142,0.0929962794981221,0.0122221513424288,0.0495100179460231,0.0959626510640031)
uvmeanonethridRe0550HJ(x)=-f15(x,-1.58957890152675e-05,0.00935492568149067,0.0904621607225798,0.0117681062374765,0.0463835645296073,0.10876447729061)
uvmeanonethridRe0180HJ(x)=-f15(x,-4.13115872958601e-05,0.00634117288335139,0.0750839076181533,0.00949281371640684,0.0311579741625425,0.225915980134867)
uvmeanRe5200LM(x)=uvmeanonethridRe5200LM(x)**3
uvmeanRe2000LM(x)=uvmeanonethridRe2000LM(x)**3
uvmeanRe1000LM(x)=uvmeanonethridRe1000LM(x)**3
uvmeanRe0550LM(x)=uvmeanonethridRe0550LM(x)**3
uvmeanRe0180LM(x)=uvmeanonethridRe0180LM(x)**3
uvmeanRe2000HJ(x)=uvmeanonethridRe2000HJ(x)**3
uvmeanRe0950HJ(x)=uvmeanonethridRe0950HJ(x)**3
uvmeanRe0550HJ(x)=uvmeanonethridRe0550HJ(x)**3
uvmeanRe0180HJ(x)=uvmeanonethridRe0180HJ(x)**3

```

## References

1. Hoyas, S. & Jiménez, J. 2006 Scaling of the velocity fluctuations in turbulent channels up to  $Re_\tau = 2003$ . *Phys. Fluids* **18** (011702).
2. Lee, M. & Moser, R. D. 2015 Direct numerical simulation of turbulent channel flow up to  $Re_\tau = 5200$ . *J. Fluid Mech.* **774**.